

Original Article: Oncology Nanomedicine

Nanocryosurgery and its mechanisms for enhancing freezing efficiency of tumor tissues

Jing-Fu Yan, PhD (C),^a Jing Liu PhD, BS, BE^{a,b,*}

^a*Cryogenics Laboratory, Technical Institute of Physics and Chemistry, Chinese Academy of Sciences, Beijing, China*

^b*Department of Biomedical Engineering, School of Medicine, Tsinghua University, Beijing, China*

Abstract

We proposed for the first time a surgical term, the nanocryosurgery, for efficient tumor treatment through combining the theories of cryosurgery and nanotechnology. Simulations were performed on the combined phase change bioheat transfer problems in a single cell level and its surrounding tissues, to explicate the difference of transient temperature response between conventional cryosurgery and nanocryosurgery. According to theoretical interpretation and existing experimental measurements, intentional loading of nanoparticles with high thermal conductivity into the target tissues can lower the final temperature significantly, increase the maximum freezing rate, and enlarge the ice volume obtained in the absence of nanoparticles. In addition, introduction of nanoparticle-enhanced freezing could also make conventional cryosurgery more flexible in many aspects such as artificially interfering in the size, shape, image and direction of iceball formation. The concepts of nanocryosurgery may offer new opportunities for future tumor treatment.
© 2008 Elsevier Inc. All rights reserved.

Key words:

Nanocryosurgery; Bioheat transfer; Cryoinjury; Ice nucleation; Tumor treatment

Background

Cryosurgery is a technique that uses freezing to destroy undesired tissues. This therapy is becoming popular because of its important clinical advantages. Besides being less invasive than traditional surgical resection, it minimizes pain, bleeding, and other complications of surgery, is less expensive than other treatments, and requires a much shorter recovery time and hospital stay. Although it still cannot be regarded as a routine method of cancer treatment, cryosurgery is developing rapidly as an

alternative to traditional therapies. Accompanied with modern imaging technology, the field of cryosurgery has in fact been widely extended since its early stage.¹⁻³ However, in many clinical cases it has been found that freezing alone could not completely destroy the targeted tumor; moreover, there is always a high recurrence rate with follow-up surveys.^{4,5} From the viewpoint of cryomedical engineering,⁶ the major reason concerns the freezing rate, which does not produce a massive ice nucleation in tumor cells, especially at the edge of the tumor; thus the procedure cannot guarantee complete lethality to all of the tumor. Consequently, a major concern in conventional cryosurgery is to avoid insufficient freezing between multiple cryoprobes and to maximize the freezing efficiency so as to enhance killing of the target tumor.

If cryosurgery is to be successful, freezing efficiency should be guaranteed by introducing adjuvant approaches. Belonging to the same category of physical therapy, modern hyperthermia combined with advanced nanotechnology exemplifies such endeavors. The newly developed

Received 11 March 2007; accepted 13 November 2007.

No conflict of interest was reported by the authors of this paper.

This research is partially supported by the National Natural Science Foundation of China under Grants 50575219 and 50325622.

*Corresponding author: Cryogenics Laboratory, Technical Institute of Physics and Chemistry, Chinese Academy of Sciences, Beijing 100080, China.

E-mail address: jliu@cl.cryo.ac.cn (J. Liu).

1549-9634/\$ – see front matter © 2008 Elsevier Inc. All rights reserved.

doi:[10.1016/j.nano.2007.11.002](https://doi.org/10.1016/j.nano.2007.11.002)

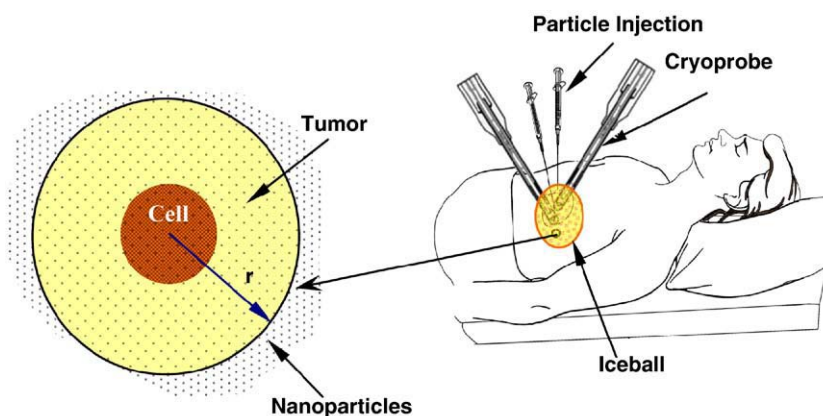


Figure 1. Schematic illustration of computational domain loaded with nanoparticles during cryosurgery (not to scale).

magnetic nanohyperthermia, which takes full advantage of electromagnetic heating effects and powerful thermosmosis, offers some attractive possibilities in tumor therapy.⁷⁻¹² Moreover, the ability to treat cancer by targeted delivery through angiogenesis or some antineoplastic drug, especially using hyperthermia-introduced nanoparticles, has also been reported to show a good treatment effect.¹³⁻¹⁵ Inspired by such curative trends in hyperthermia, we propose a new modality in cryosurgery, named nanocryosurgery, and offer our preliminary results in this article.

Methods

Basic principle of nanocryosurgery

This physical therapy is combined with advanced nanotechnologies. Its basic principle is to introduce a functional solution with nanoparticles into the target tissues (Figure 1), which then serves to maximize freezing heat transfer, increase the probability of intracellular ice formation (PIF), and regulate iceball formation orientation. Nanoparticles with high thermal conductivity allow cryosurgery to take full advantage of the enhanced heat conduction effects and their ability to serve as nucleation seeds. As was recently realized, liquids containing metallic or nonmetallic solid nanoparticles show an increase in thermal conductivity compared with that of the base liquid.^{16,17} This can also be true when applied to nanocryosurgery, where addition of metal nanoparticles into the wet biological environment will increase the tissue conductivity, which in turn results in significant freezing effects. Meanwhile, according to the theory of ice nucleation, it will be seen that massive loading of nanoparticles in tumor cells is bound to induce more efficient heterogeneous nucleation as ice seeds, which to some extent guarantees a higher PIF, the main reason for cell death in cryosurgery.¹⁸⁻²⁰

Moreover, because the particulate suspension can be locally injected and distributed into the region of interest as desired,²¹ it is available to provide accurate killing on the nanoscale by means of nanocryosurgery. As is well known, freezing affects biological systems at both nanoscale (molecular) and microscale (cellular) levels, which may bring about changes in structure, composition, water and fat content, and salinity of tissues.^{3,22} High concentrations of nanoparticles combined with freezing might enhance such harmful effects. Although a series of studies²³⁻²⁵ have been published on the toxicological effect of nanoparticles, the potential toxicity to normal tissues with targeted injection of particles could be prevented through appropriate choice of particle type and careful control of injection time, procedure, and dose of particulate suspension. Thus far, it is clear that some candidate particles like the iron oxide magnetite (Fe_3O_4) and gold (Au), have good biological compatibility and have been widely used in clinics. Meanwhile, using nanoparticles to deliver antineoplastic drugs or angiogenesis to damage target tumors has also proved feasible for tumor treatment. For instance, Bischof and colleagues¹⁵ proposed a novel method using Au nanoparticle-assisted tumor necrosis factor- α delivery in combination with hyperthermia, which significantly delayed tumor growth, reducing both tumor cell survival rate and tumor blood perfusion. All of these working media and techniques can also be used in nanocryosurgery.

Furthermore, the iceball growth during cryosurgery can be artificially controlled by asymmetrically injecting nanoparticle solution into the targeted tissues, thus making cryosurgery more flexible. It is often difficult to produce an optimal cryolesion area using conventional cryosurgical technique because of the irregular shape of the tumor. However, when using injected nanoparticles the growth state of ice crystals can be efficiently modified as desired. In nanocryosurgery one can regulate growth direction and orientation of an iceball, thus permitting good conformation of the cryosurgery to the tumor outline.

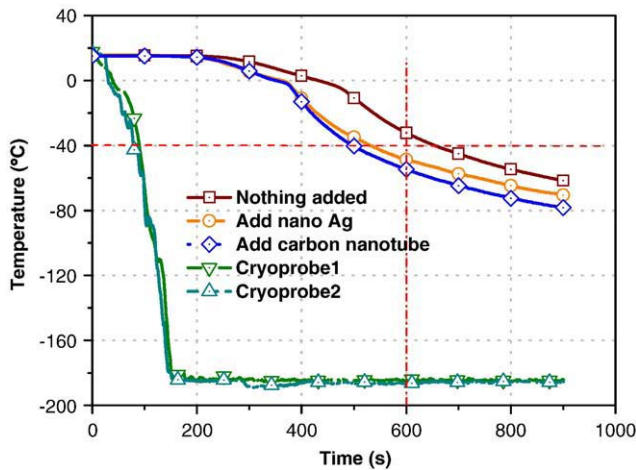


Figure 2. Transient temperature response of selected position with different injection samples during same freezing process.

Finally, introduction of nanoparticles into target tissues could improve image contrast and offer a better image guidance for the cryosurgical operation.²⁶ In this respect, some imaging magnetic nanoparticles²⁷ such as Fe_3O_4 , 20–30 nm in diameter, have been found to increase the resolution and contrast of several commonly used imaging techniques in minimally invasive therapy such as magnetomotive optical coherence tomography or magnetic resonance imaging. Fluorescent nanoparticles are also used as image probes to image and monitor thermal lesion of tissue during thermal therapies so as to guarantee an accurate treatment.²⁸ Such characteristics of nanoparticles can increase the curative tumor-killing effect and decrease local recurrence rate as well. Therefore, when nanotechnology meets cryosurgery, the treatment efficiency of conventional cryosurgery is expected to be significantly improved.

Experimental findings for nanocryosurgery

Several experiments already performed in our laboratory have demonstrated the significant effect of nanoparticles in enhancing the process of freezing biological tissues. According to the typical temperature response curves of pork tissue during the freezing process with one liquid nitrogen-based cryoprobe,²¹ it has been shown that the lowest temperature for injecting nanoparticles (30 mL 5% w/w particulate suspension) can reach -115°C at a location 5 mm distant from the probe, which is much lower than its counterpart case of no injection. The latter case achieves only a lowest temperature of -75°C at the same position and under the same freezing conditions. This was a result of the enhanced heat conduction due to the addition of metal nanoparticles into tissues. Presented in Figure 2 is a newly obtained transient temperature response of the selected position (at the midpoint between two liquid nitrogen cryoprobes spaced 2 cm apart) during the same freezing

process based on three different conditions. Nano-silver was added in a phantom gel as case 1, and carbon nanotubes as case 2, whereas the original phantom gel was referred as the reference sample. From the curve it can be seen that the freezing rate at the target position where nanoparticle solutions were locally injected was evidently increased. Generally, if the freezing process does not endure long enough, it could lead to a “dead region” representing insufficient freezing between two cryoprobes (as indicated by red dotted lines in Figure 2). Clearly, with the help of nanoparticle-enhanced freezing, such dead regions could be successfully prevented. In other words, the possibility of insufficient freezing will be decreased substantially.

To evaluate the capacity for controlling the size, shape, and direction of the iceball formation by injecting nanoparticle solutions with specific thermal properties into the target tissues, we had adopted a medical infrared thermometer to map the temperature profile over the whole surface above the freezing area.¹⁸ In a typical test, different volumes of particulate solution were considered. As thermal images indicated, different doses of injecting solution have resulted in varied magnitudes of iceball formation, which indicates that the appropriate particulate solution could effectively regulate the tumor-killing area via directional freezing.

Bioheat transfer model

Nanoparticle-aided cryosurgery can produce a predictable improvement of temperature response on the target tissue and cell. Because the present study focuses only on the freezing effect of a single tumor cell when different kinds of nanoparticles have already been injected in or outside the cell membranes, the computational domain can be simplified and depicted in Figure 1, which is divided into two parts: intracellular and extracellular areas. For simplicity, a spherical coordinate system in one dimension was used. Calculations of heat transfer are based on the widely accepted bioheat model proposed by Pennes,²⁹ which is widely used in the description of the tissue freezing process.

In the intracellular medium the bioheat equation is expressed as follows:

$$C \frac{\partial T}{\partial t} = k_i \cdot \frac{1}{r} \cdot \frac{\partial^2(rT)}{\partial r^2} + Q_m \quad (1)$$

In the extracellular medium the effect of blood perfusion should be included, and the bioheat equation reads as:

$$C \frac{\partial T}{\partial t} = k_o \cdot \frac{1}{r} \cdot \frac{\partial^2(rT)}{\partial r^2} + \omega_b C_b (T_a - T) + Q_m \quad (2)$$

where T is the temperature, C_b and ω_b are the heat capacity and the blood perfusion of biological tissues, respectively; k_i and k_o are intracellular and extracellular thermal conductivity, respectively; C is heat capacity of biomaterial including the contribution of the loaded nanoparticles; Q_m is the metabolic heat generation, and T_a is arterial temperature.

Table 1
Physical properties of biological tissues and nanoparticles^{30–32}

| Items | Units | Values |
|---|---------------------|--------------------|
| Thermal conductivity of frozen tissue, k_{ft} | W/m °C | 2 |
| Thermal conductivity of unfrozen tissue, k_{ut} | W/m °C | 0.5 |
| Thermal conductivity of Al_2O_3 , k_p | W/m °C | 39.7 |
| Heat capacity of Al_2O_3 , C_p | J/m °C | 2.82×10^6 |
| Thermal conductivity of Fe_3O_4 , k_p | W/m °C | 7.1 |
| Heat capacity of Fe_3O_4 , C_p | J/m °C | 3.2×10^6 |
| Thermal conductivity of Au, k_p | W/m °C | 297.73 |
| Heat capacity of Au, C_p | J/m ³ °C | 2.21×10^6 |
| Thermal conductivity of PTFE, k_p | W/m °C | 0.2 |
| Heat capacity of PTFE, C_p | J/m °C | 2.13×10^6 |
| Thermal conductivity of diamond, k_p | W/m °C | 2000 |
| Heat capacity of diamond, C_p | J/m °C | 1.4×10^6 |
| Heat capacity of frozen tissue, C_{ft} | J/m °C | 2×10^6 |
| Heat capacity of blood, C_b | J/m °C | 3.6×10^6 |
| Heat capacity of unfrozen tissue, C_{ut} | J/m °C | 3.6×10^6 |
| Latent heat, L | J/m °C | 250×10^6 |
| Temperature of lower phase change, T_l | K | 265.15 |
| Temperature of upper phase change, T_u | K | 272.15 |
| Temperature of outside boundary, T_p | K | 77 |
| Arterial temperature, T_a | K | 310.15 |

The mathematical model used here is based on four principal assumptions: (1) The effect of cell deformation due to freezing is neglected, and the transmembrane temperature difference is also omitted for simplicity. (2) Both the target cell and its surrounding tumor area are regarded as an ideal sphere, and the media inside or outside the cell as homogeneous and are treated as one-dimensional. (3) The thermal properties of nanoparticles are treated as temperature-independent. (4) The injected nanoparticles are all treated as ideal spheres.

Because the Hamilton-Crosser (H-C) model is the classical theory to predict thermal conductivity of nanofluids that has been applied in the field of particles-tissue interaction resulting from hyperthermia, in this study it is also used for calculating the thermal conductivities of objects composed of biomaterials and nanoparticles. Another reason to use the H-C model is that it can simply but effectively describe the macroscale thermal conductivity of nanoparticle-tissue mixtures without considering the size effect of nanoparticles, which, according to our previous experimental results, does not play a distinct role in increasing the macroscale thermal conductivity.

Considering phase change phenomena during cryosurgery, the effective heat capacity method is adopted to simultaneously solve the heat transfer in frozen and unfrozen areas. According to the H-C model, in frozen and unfrozen

areas, the thermal conductivity for the treated object can be depicted, respectively, as follows:

$$k_f = k_{ft} \cdot \frac{k_p + 2k_{ft} - 2\eta(k_{ft} - k_p)}{k_p + 2k_{ft} + \eta(k_{ft} - k_p)} \quad (3)$$

$$k_u = k_{ut} \cdot \frac{k_p + 2k_{ut} - 2\eta(k_{ut} - k_p)}{k_p + 2k_{ut} + \eta(k_{ut} - k_p)} \quad (4)$$

As for thermal capacity, considering the energy equation for a two-component (biology part and nanoparticle part) system of biomaterial, the volume fraction of particle used in Equations (3) and (4) is introduced. Then the thermal capacity can be defined as follows:

$$C_f = C_{ft} \cdot (1 - \eta) + C_p \cdot \eta \quad (5)$$

$$C_u = C_{ut} \cdot (1 - \eta) + C_p \cdot \eta \quad (6)$$

here, subscripts f and u represent frozen and unfrozen mixture, respectively. Subscripts ft and ut mean frozen and unfrozen tissues, respectively. Subscript p stands for the loaded particles.

Based on Equations (1) and (2), a unified equation, which can be applied to frozen, partially frozen, and unfrozen tissue regions, can be written by introducing effective heat capacity. Because the phase change of real biological tissue does not take place at a specific temperature but within a temperature range, it is reasonable to substitute a large effective heat capacity over a temperature range (T_{ml} , T_{mu}) for the latent heat, where T_{ml} and T_{mu} are, respectively, the lower and upper phase transition temperatures of the tissue. For brevity, the derivation and definition of effective thermal capacity, effective thermal conductivity, effective metabolic heat generation, and effective blood perfusion are not repeated here. Readers are referred to Deng and Liu²⁹ for more details.

Results

Simulation results

Considering the typical characteristic size of biological cells as between 5 and 20 μm , the radius of a tumor cell is taken here as 10 μm . It is assumed further that the distance between the cell center and the boundary of the calculation domain is 30 μm . For simplification, only the first boundary condition was considered, namely to suppose that $T = 77$ K at the edge of the calculation domain. For much more complicated situations the present method is still applicable. In addition, the initial temperature in the calculation domain is set as $T = 310.15$ K.

The theoretical model was simulated using the finite element method. Typical properties for biological tissue^{30,31} as well as different kinds of particles³² are listed in Table 1 in the following simulations. Considering that the size effect of nanoparticles is neglected with the H-C model and has

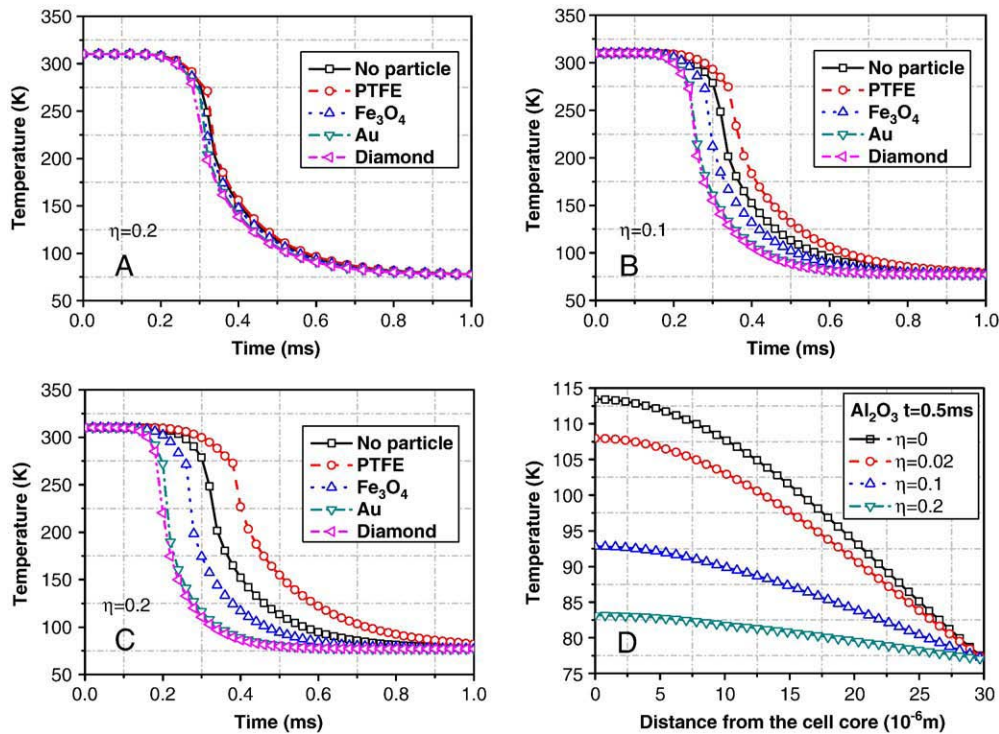


Figure 3. Freezing temperature responses at the core of the studied cell for different nanoparticle loading situations where the volume fraction of particles is distributed uniformly by $\eta = 1\%$ within the cell interior and outside the cell by $\eta = 2\%$ (A), $\eta = 10\%$ (B), and $\eta = 20\%$ (C), respectively. (D) Temperature profile along the radius direction at 0.5 ms with different concentrations of nano- Al_2O_3 .

minimal influence on the macroscale thermal conductivity as mentioned, standard thermal property values for particles are used instead.

Presented in Figure 3, A–C are the temperature responses at the core of a cell during freezing for the situations loading with different kinds of nanoparticles when their volume fractions are $\eta = 1\%$ in the cell and $\eta = 2\%$, $\eta = 10\%$, and $\eta = 20\%$ outside the cell, respectively. Figure 3, D shows the temperature profile along the radius direction at 0.5 ms with different concentrations of nano- Al_2O_3 . It can be seen that different kinds and concentrations of nanoparticles have different influences on the freezing rate in the cell. A large volume fraction of nanoparticles with high thermal conductivity could evidently increase the freezing rate of the cell. On the contrary, particles with low thermal conductivity could decrease the freezing rate. As shown from Figure 3, A–C, at the same volume fraction, polytetrafluoroethylene (PTFE) and diamond play a much more significant role in affecting the freezing rate than other candidate particles. This can be attributed to their lowest and highest thermal conductivity, respectively. However, from Figure 3, A–C it was shown that at one volume fraction there would be a limitation on the increase in freezing rate when using particles with larger thermal conductivity. That is, concentrations correlate closely with thermal conductivities of particles in the contribution to freezing enhancement. For instance, although diamond has a thermal conductivity

exceeding that of gold by fivefold, it is noted that if its volumetric loads are not high enough there is almost no differential cooling effect with nanogold. Therefore, choosing an optimal concentration with appropriate particles is crucial to maximize the effects of cryosurgery with minimum cost. In addition, with the increase of volume fractions in tumor cells, the influence induced by particles becomes stronger and more apparent. Figure 3, D shows that the temperature of a tumor cell core with a 20% volume fraction of nano- Al_2O_3 could decrease to 82 K at 0.5 ms, whereas it could only reach 107 K with 2% volumetric loads. However, it still can be observed that the freezing enhancement induced by a 2% volume fraction of nano- Al_2O_3 is evident in comparison with the case without loading nanoparticles (6 K temperature difference in core of cell at 0.5 ms). As can be seen in Figure 3, D, the calculated values are in good accord with the currently available experimental data.²¹

To better quantify the freezing rate of a cell loaded with nanoparticles, Figure 4, A–C, corresponding to the same situations in Figure 3, A–C, presents the freezing rate response at the core of the cell, with maximum freezing rates specifically marked on the curve. At the same time, an average temperature-decreasing rate at the core of the cell can be defined as $-B = \frac{1}{\tau} \int_0^\tau \frac{\partial T}{\partial t} dt$, where τ is the freezing time. Here the total freezing time is calculated as 1 ms, because the freezing procedure tends to be relatively stable

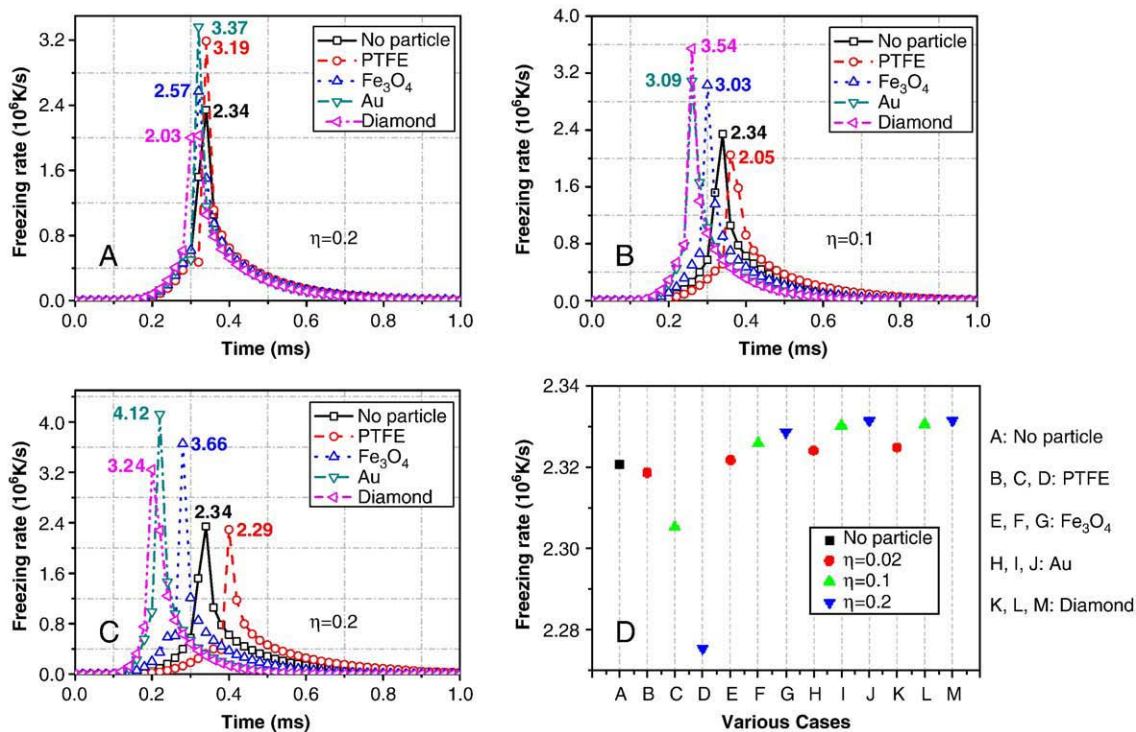


Figure 4. Freezing-rate response at the core of the cell, where the maximum rate was marked. Here, A to C correspond to Figure 3, A–C, respectively. D, Average temperature decreasing rate at the core of the cell with various particle loading fractions and particle types.

after that. The results are illustrated in Figure 4, D for various cases. An interesting result can be found in Figure 4, A–C that at the same concentration of particles, the time of maximum freezing rate occurs in accordance with the order of thermal conductivity. Diamond, with greatest thermal conductivity, results in the earliest maximum freezing rate, whereas PTFE results in the last one. However, it seems that the actual value of the maximum freezing rate has no clear correlation with the kinds and volume fractions of particles. As shown from Figure 4, A–C, the maximum freezing rate of Au could reach 3.37×10^6 K/s and 4.12×10^6 K/s when the fraction volume outside the cell is 0.02 and 0.2, respectively, whereas the maximum freezing rate will only reach 3.09×10^6 K/s when its fraction volume is 0.1. Meanwhile, it can also be seen that when $\eta = 20\%$, the best thermal conductivity particles (diamond) do not necessarily guarantee reaching a maximum freezing rate, as reflected by Figure 4, C. Therefore, one can conclude that the maximum freezing rate not only depends on the thermal conductivities but also on the volume fraction and other thermal properties such as density, heat capacity, and latent heat. As for the average freezing rate in Figure 4, D, it demonstrates effectively that the better thermal conductivity and the larger volume fraction it has, the higher value of average freezing rate it could reach. It can be found that the maximum average freezing rate reaches about 2.33×10^5 K/s when diamond is used and $\eta = 20\%$ outside the cell, and the increasing magnitude attains about 2.5% compared with the PTFE state. Likewise, the maximum magnitude of maximum freezing rate can reach 76% when

Au is used and $\eta = 20\%$ outside the cell compared with the no-particle case. Therefore, from the above discussion it is clear that nanocryosurgery could produce stronger freezing effects than that of conventional cryosurgery, especially with regard to the maximum freezing rate. Such influence is very important in a large extent to enhance killing of tumor tissues during cryosurgery.

Nucleation mechanism of nanocryosurgery

From the above heat transfer simulation it can be seen that the maximum freezing rate could be substantially improved when nanoparticles are introduced. However, this is still not the complete story, because the temperature decrease alone does not necessarily represent that the tumor cell has become necrotic. Besides their influence on freezing speed, nanoparticles also play an important role in inducing ice nucleation, which is critical in determining the final cell damage. As will be illustrated in the following, using nanoparticles as seeds, the heterogeneous nucleation rate could be significantly improved. Such an improvement results in a higher PIF, leading to a lethal effect on tumor cells.

In a classical homogeneous nucleation theory, the standard Gibbs free energy of formation (ΔG_i) of a cluster of phase β (ice) containing i molecules from its mother phase α is given by:³³

$$\Delta G_i = i v^\beta \Delta G_i + (36\pi)^{1/3} i^{2/3} \sigma^{\alpha\beta} (v^\beta)^{2/3} \quad (7)$$

where ΔG_i is the Gibbs free-energy difference between α and β phase per volume, v^β is the molecular volume of phase

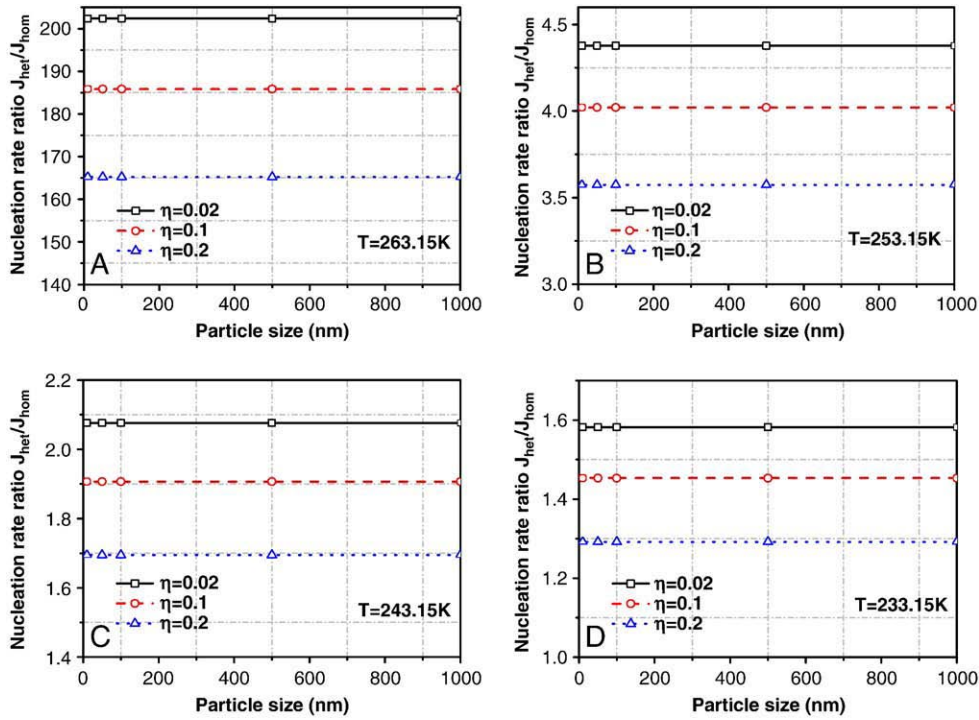


Figure 5. The influence of particle size and volume fractions upon nucleation effectiveness at different temperatures.

β , and $\sigma^{\alpha\beta}$ is the interfacial free energy per unit area. Maximizing ΔG_i with respect to i and assuming closely packed water molecules, one can obtain the following relationships for the critical cluster:

$$i^* = -\frac{32\pi}{3\nu\beta} \left[\frac{\sigma^{\alpha\beta}}{\Delta G_t} \right]^3, \quad \text{or} \quad r^* = -\frac{2\sigma^{\alpha\beta}}{\Delta G_t} \quad (8)$$

and the following relationship for ΔG_{i^*} :

$$\Delta G_{i^*} = \frac{16\pi}{3} \frac{(\sigma^{\alpha\beta})^3}{(\Delta G_t)^2} \quad (9)$$

where r^* is the radius of the critical cluster.

Considering both diffusion barrier $\Delta G_{i'}$ and nucleation barrier ΔG_{i^*} , nucleation rate J_{hom} reads as³⁴:

$$J_{\text{hom}} = \frac{n_1 kT}{h} \exp\left(-\frac{\Delta G_{i'}}{kT}\right) \exp\left(-\frac{\Delta G_{i^*}}{kT}\right) \quad (10)$$

where h is Planck's constant, k the Boltzmann constant, and n_1 molecules per unit volume of mother phase.

When nanoparticles are introduced as seeds and uniformly distributed throughout the target tissue or cell, the heterogeneous nucleation will play a leading role. According to heterogeneous nucleation theory, r^* and ΔG_{i^*} are respectively given by:

$$r^* = -\frac{2\sigma^{\alpha\beta}}{\Delta G_t} \quad (11)$$

$$\Delta G_{i^*} = \frac{8\pi\sigma^{\alpha\beta}}{3(\Delta G_t)^2} f(\eta, x) \quad (12)$$

here, x is defined as $x = R_n/r^*$, R_n is the radius of the particle. $\eta = \cos\theta$, in which θ is the wrapping angle. Because it is assumed that particles in the cell are in the state of perfect humidification, that is $\theta = 0$ and $\eta = 1$. Therefore, $f(\eta, x)$ can be expressed as follows³⁵:

$$f(\eta, x) = 1 + \left(\frac{1-x}{g}\right)^3 + x^3 \left[2 - 3\left(\frac{x-1}{g}\right) + \left(\frac{x-1}{g}\right)^3 \right] + 3x^2 \left(\frac{x-1}{g} - 1\right) \quad (13)$$

where, $g = (1+x^2-2x)^{1/2}$.

As is well known, the heterogeneous nucleation rate J_{het} can be defined as:

$$J_{\text{het}} = \frac{n_0 kT}{h} 4\pi R_n^2 \exp\left(-\frac{\Delta G_{i'}}{kT}\right) \exp\left(-\frac{\Delta G_{i^*}}{kT}\right) \quad (14)$$

where n_0 is number of water molecules contacting the particle surface per unit area.

If homogeneous nucleation is the main process in the no-particle case, whereas heterogeneous nucleation is the main process in particle case, under the same temperature

condition, the nucleation rate ratio that implies the influence of particles on ice nucleation can be obtained as follows:

$$J_{\text{het}}/J_{\text{hom}} = \frac{n_0 \cdot 4\pi R_n^2}{n_1} \exp\left(\frac{8\pi\sigma^{\alpha\beta}}{3kT(\Delta G_t)^2} \left(2(\sigma^{\alpha\beta})^2 - f(1, x)\right)\right). \quad (15)$$

Because of the lack of experimental data, in this study we assume that $r^* = 1 \text{ nm}$, $\sigma^{\alpha\beta} = 2 \text{ mJ/m}^2$, $\Delta G_t = -1E10^3 \text{ T}$ (273.15-T), $\frac{n_0 \cdot 4\pi R_n^2}{n_1} = 1 - \eta$, and Figure 5 quantitatively depicts the influence of particle size and volume fractions upon nucleation effectiveness. From the calculation as given in Figure 5, A–D, it can be seen that once nanoparticles are loaded into the cell, the heterogeneous nucleation rate would be significantly high at the beginning of the freezing process in comparison with the no-particle case, which implies that nanocryosurgery could result in cell death at a relatively high temperature threshold. In addition, if particle size exceeds the radius of the critical cluster, its influence on ice nucleation does not change. However, it is interesting to note that particles with low volume fraction can increase the nucleation rate much more than the ones with high volume fraction. This is a contradiction when considering freezing enhancement. Consequently, the optimal relationship between appropriate particle size, concentration, and freezing process in ice nucleation to maximize cell death should be further studied.

Discussion

In addition to enhancing the freezing strength to kill targeted tumors, nanocryosurgery can also reduce freezing injury to normal tissues around the tumor focus. In addition to metals, nanoparticles can be composed of biodegradable polymer, liposome, micelle, drug and semiconductor, etc. Magnetic microparticles and nanoparticles have been applied in hyperthermia in several ways including the formation of glass ceramics, microcapsules, or suspensions. The amount of material required to produce the desired temperatures depends on the particle delivery method¹⁰ (e.g., mainline, arterial injection, hypodermic injection, and direct injection), which will affect the final output of the nanocryosurgery. In addition, during the freezing process the tumor vessels quickly and substantially dilate and increase in permeability, hence concentrating the particulate suspension in the tumor but not in normal tissue. The same mechanism has been successfully applied in cryochemotherapy and should be equally applicable in nanocryosurgery. Thus, the toxicity of particles resulting from high concentrations is lethal mainly to targeted tumors and not normal tissues, provided that the particle injection time, procedure, and dose of particulate suspension are well controlled.

With respect to the choice of particle for enhancing freezing, magnetite (Fe_3O_4) and diamond are perhaps the most popular and appropriate because of their good

biological compatibility. Particle sizes less than $10 \mu\text{m}$ are normally considered sufficiently small to permit effective delivery to the site of the tumor, either via encapsulation in a larger moiety or suspension in a carrier fluid. Introduction of nanoparticles into the target would effectively increase the nucleation rate at a high temperature threshold. In this case, a cryoprobe with only a moderate freezing capability may work well for treating the tumor.

Although a complete understanding of nanocryosurgery is presently not yet available, this study offers a preliminary outline of the new therapy's promising future. Such a surgical protocol could overcome the limitations of conventional cryosurgery in many respects and offers a much higher maximum freezing rate as well as possibilities of ice nucleation. It can also be helpful and flexible for an adaptive tumor treatment as well as in vivo medical imaging. In an ideal scenario, a minimally invasive and safe freezing therapy could be guaranteed. Future efforts should be directed toward both the fundamental mechanisms as well as clinical issues of the new conceptual nanocryosurgery.

References

1. Rubinsky B. Cryosurgery: advances in the application of low temperatures to medicine. *Int J Refrig* 1991;14:190-9.
2. Gage AA. Cryosurgery in the treatment of cancer. *Surg Gynecol Obstet* 1992;174:73-92.
3. Rubinsky B. Cryosurgery. *Annu Rev Biomed Eng* 2000;2:157-87.
4. Izawa JI, Madsen LT, Scott SM, Tran JP, McGuire EJ, von Eschenbach AC, et al. Salvage cryotherapy for recurrent prostate cancer after radiotherapy: variables affecting patient outcome. *J Clin Oncol* 2002;20:2664-71.
5. Seifert JK, Springer A, Baier P, Junginger T. Liver resection or cryotherapy for colorectal liver metastases: a prospective case control study. *Int J Colorectal Dis* 2005;20:507-20.
6. Bourne MH, Piepkorn MW, Clayton F, Leonard LG. Analysis of microvascular changes in frostbite injury. *J Surg Res* 1986;40:26-35.
7. Jordan A, Wust P, Scholz R, Tesche B, Fahling H, Mitrovics T, et al. Cellular uptake of magnetic fluid particles and their effects on human adenocarcinoma cells exposed to AC magnetic fields in vitro. *Int J Hyperthermia* 1996;12:705-22.
8. Johannsen M, Gneveckow U, Eckelt L, Feussner A, Waldofner N, Scholz R, et al. Clinical hyperthermia of prostate cancer using magnetic nanoparticles: presentation of a new interstitial technique. *Int J Hyperthermia* 2005;21:637-47.
9. Johannsen M, Thiesen B, Gneveckow U, Taymoorian K, Waldofner N, Scholz R, et al. Thermotherapy using magnetic nanoparticles combined with external radiation in an orthotopic rat model of prostate cancer. *Prostate* 2006;66:97-104.
10. Lv YG, Deng ZS, Liu J. Study on the induced heating effects of embedded micro/nano particles on human body subject to external medical electromagnetic field. *IEEE Trans Nanobioscience* 2005;4:284-94.
11. Zhao DL, Zhang HL, Zeng XW, Xia QS, Tang JT. Inductive heat property of Fe_3O_4 /polymer composite nanoparticles in an AC magnetic field for localized hyperthermia. *Biomed Mater* 2006;1:198-201.
12. Andreas J, Regina S, Klaus MH, Manfred J, Peter M, Jacek N, et al. Presentation of a new magnetic field therapy system for the treatment of human solid tumors with magnetic fluid hyperthermia. *J Magn Mater* 2001;225:118-26.
13. Kong G, Braun RD, Dewhirst MW. Hyperthermia enables tumor-specific nanoparticle delivery: effect of particle size. *Cancer Res* 2000; 60:4440-5.

14. Brannon PL, Blanchette JO. Nanoparticle and targeted systems for cancer therapy. *Adv Drug Deliv Rev* 2004;56:1649-59.
15. Visaria RK, Griffin RJ, Williams BW, Ebbini ES, Paciotti GF, Song CW, et al. Enhancement of tumor thermal therapy using gold nanoparticle-assisted tumor necrosis factor- α delivery. *Mol Cancer Ther* 2006;5:1014-20.
16. Xu J, Yu BM, Zou MQ, Xu P. A new model for heat conduction of nanofluids based on fractal distributions of nanoparticles. *J Phys D Appl Phys* 2006;39:4486-90.
17. Zhang X, Gu H, Fujii M. Experimental study on the effective thermal conductivity and thermal diffusivity of nanofluids. *Int J Thermophys* 2006;27:569-80.
18. Yan JF, Liu J, Zhou YX. Infrared image to evaluate the selective (directional) freezing due to localized injection of thermally important solutions. 27th Annual International Conference of the IEEE Engineering in Medicine and Biology Society (EMBS). Shanghai, China; 2005.
19. Mazur P. The role of intracellular freezing in the death of cells cooled at supraoptimal rates. *Cryobiology* 1977;14:251-72.
20. Toner M. Nucleation of ice crystals inside biological cells. In: Steponkus P, editor. *Advances in low-temperature biology*. London: JAI Press; 1993. p. 1-51.
21. Yu TH, Liu J, Zhou YX. Selective freezing of target biological tissues after injection of solutions with specific thermal properties. *Cryobiology* 2005;50:174-82.
22. Gage AA, Baust JG. Mechanisms of tissue injury in cryosurgery. *Cryobiology* 1998;37:171-86.
23. Dreher KL. Health and environmental impact of nanotechnology: toxicological assessment of manufactured nanoparticles. *Toxicol Sci* 2004;77:3-5.
24. Nel A, Xia T, Mädler L, Li N. Toxic potential of materials at the nanolevel. *Science* 2006;311:622-7.
25. Jenkins J, Pant K, Hood J, Sundaram S. Multi-scale, mechano-biological model of nanoparticle toxicity. *Nanotechnol* 2006;1:599-602.
26. Wickline SA, Lanza GM. Nanotechnology for molecular imaging and targeted therapy. *Circulation* 2003;107:1092-5.
27. Amy O, Farah T, Kenneth S, Alexander W, Stephen B. Magnetomotive contrast for in vivo optical coherence tomography. *Opt Express* 2005;13:6597-614.
28. <http://mae.uta.edu/~bhan/research.html>.
29. Deng ZS, Liu J. Numerical simulation on 3-D freezing and heating problems for the combined cryosurgery and hyperthermia therapy. *Numer Heat Transf A Appl* 2004;46:587-611.
30. Rabin Y, Shitzer A. Numerical solution of the multidimensional freezing problem during cryosurgery. *ASME J Biomech Eng* 1998;120:32-7.
31. Chato JC. Selected thermophysical properties of biological materials. In: Shitzer A, Eberhart EC, editors. *Heat transfer in medicine and biology*. New York: Plenum Press; 1985. p. 413-8.
32. Ma QF. *Practical thermal properties handbook*. Beijing: Chinese Agriculture and Mechanic Press; 1986. p. 144-76.
33. Toner M, Cravalho EG. Thermodynamics and kinetics of intracellular ice formation during freezing of biological cells. *J Appl Phys* 1990;67:1582-94.
34. Turnbull D. Under what conditions can a glass be formed. *Contemp Phys* 1969;10:473-88.
35. Taylor MJ. *Physico-chemical principles in low temperature biology*. In: Grout BWW, Morris GJ, editors. *The effect of low temperature on biological systems*. Chicago: Edward Arnold; 1987. p. 3-71.